The ferromagnetic behaviour of conducting polymers revisited

2008 J. Phys.: Condens. Matter 20 035214

(http://iopscience.iop.org/0953-8984/20/3/035214)

J. Phys.: Condens. Matter **20** (2008) 035214 (8pp) doi:10.1088/0953-8984/20/03/035214

The ferromagnetic behaviour of conducting polymers revisited

O R Nascimento[1], A J A de Oliveira[2], E C Pereira[3], A A Correa[3] and L Walmsley[4]

[1] Instituto de Física de São Carlos, Universidade de São Paulo, Caixa Postal 369, CEP 13560-970, São Carlos, São Paulo, Brazil
[2] Departamento de Física, Universidade Federal de São Carlos, Caixa Postal 676, CEP 13565-905, São Carlos, São Paulo, Brazil
[3] Departamento de Química, Universidade Federal de São Carlos, Caixa Postal 676, CEP 13560-970, São Carlos, São Paulo, Brazil
[4] Departamento de Física, Instituto de Geociências e Ciências Exatas, Universidade Estadual Paulista, Caixa Postal 178, CEP 13500-970, Rio Claro, São Paulo, Brazil

E-mail: walmsley@rc.unesp.br

Received 22 June 2007, in final form 8 November 2007
Published 17 December 2007
Online at stacks.iop.org/JPhysCM/20/035214

Abstract
The magnetic properties of doped pellets of poly(3-methylthiophene) showing room temperature ferromagnetic behaviour have been discussed in a previous article. The magnetic behaviour was attributed to a weak ferromagnetic phase, due to the superexchange interaction of polarons via the dopant anions. The Dzialoshinsky–Morya interaction among canted spins was proposed to explain the ferromagnetism. In this article the main conclusions of that work concerning the magnetic behaviour are revised. The basic assumption now is that the magnetic moments are spin 1/2 polarons that can interact antiferromagnetically and/or ferromagnetically. In the small crystalline regions of the polymer, which are identified with the polymer portion that remains ferromagnetic at room temperature, the interaction gives rise to $S = 0$ and 1 bipolarons and the $S = 1$ triplet state is lower in energy. In the disordered region, disorder will prevent the complete $S = 1$ and 0 coupling and bands of polarons ferromagnetically and antiferromagnetically coupled will appear. Using this approach, all the magnetization data can be qualitatively explained, as well as the electron spin resonance data.

1. Introduction

In a recent work [1] we have reported a room temperature ferromagnetic phase in pellets of a doped sample of poly(3-methylthiophene). The sample was electrochemically synthesized in the oxidized state and partially reduced to a doping level in which the magnetic remanence was maximal. The ferromagnetic behaviour could be observed in the full range from room temperature to 5 K. Determining the number of spins 1/2 from the comparison of the room temperature electron spin resonance (ESR) intensity with a standard, we have obtained the number of spins 1/2 in excellent agreement with the number of polarons inferred from the doping level (around 5%) obtained from electron dispersive x-ray spectroscopy (EDS) measurements. Comparing the ESR and magnetization data, we have observed a remarkable difference in the behaviour with temperature of the ESR intensity compared with the magnetization temperature dependence for comparable magnetic fields. We have attributed it to the presence of antiferromagnetism and to the Dzialoshinsky–Morya mechanism for the origin of the ferromagnetism. This conclusion will now be revised by a careful analysis of the ESR and superconducting quantum interference device (SQUID) data as a function of the temperature, using as start point a model in which we separate the contribution from the small ordered part of the sample and that of the remaining disordered polymer and assume that the spin 1/2 polarons can interact ferromagnetically and/or antiferromagnetically. ESR measurements at 4.2 K in a more extended range of magnetic fields were also performed to discuss the issue of contamination.

In conducting polymers the polaronic defect is created by the extra charge introduced in the doping (intercalation) process which leads to a deformation of the chain, consisting

of a length change of the bond. In other words, breaking a double bond in the doping process introduces a positive charged defect and a dangling bond, which couple to produce the positive polaron. Calculations indicate that a positive polaron extends over six monomeric units in polythiophene [2] and over four monomeric units in polypyrrole [3]. But the question of which is the predominant defect in non-degenerate conducting polymers like polythiophene and derivatives or polypyrrole has been a challenge from the beginning of the conducting polymers research. At high doping levels calculations in the framework of the SSH (Su, Schrieffer and Heeger) Hamiltonian [4] indicate that a polaron is unstable with respect to the pairing of their spins and formation of a doubled charged spinless bipolaron [2, 3]. Fisher *et al* [5] discussed the bipolaron stability with the introduction of the electron–electron interaction. Although they conclude with the bipolaron stability, they also remark that their calculations do not take the dopant ions into account. If, from the theoretical point of view the bipolaron seems to be a more stable defect than a polaron, the experimental work has shown undoubted signatures of polaronic behaviour observed from optical measurements [6, 7] and a Curie component of the magnetic susceptibility due to localized magnetic moments observed in a variety of conducting polymers with different degrees of order and even at high doping levels [8, 9]. Kahol and Mehring [10] were the first to point out the importance of the exchange to analyse the susceptibility data in conducting polymers and proposed the exchange-coupled pair model to treat the susceptibility data in several conducting polymers. In later publications on alkyl substituted polyanilines [11] and sulfonated polyanilines [12], Kahol *et al* suggested for the first time the possibility of the contribution of magnetic bipolarons to the magnetic susceptibility data. Starting from a different approach, Mizoguchi *et al* [13] needed to introduce a spin exchange contribution to explain their spin-diffusion process in polyaniline at low temperatures. They have estimated the low temperature limiting value of the ratio of the intrachain exchange constant to the Boltzmann constant to be around 10 K. Bussac and Zuppiroli [14] have calculated singlet and triplet states of a bipolaron with the adiabatic continuum model including short range Coulomb repulsions between electrons and the attraction of the doping counterions. This model was applied by Kahol *et al* [15, 16] to analyse magnetic susceptibility data in several conducting polymers. A model of polaron clusters was also proposed by Zuppiroli *et al* [17] to explain evidence of polaron correlation observed from magnetoresistance data. Evidence of ferromagnetism at low temperature in polypyrrole films is reported in [9]. Long *et al* [18] have reported magnetic field dependent susceptibility data in polyaniline and polypyrrole nanostructures. Recently, ferrimagnetic behaviour with a critical temperature around 350 K has been reported in a new type of polymer, composed of polyaniline (PANI) and an acceptor molecule, tetracyanoquinodimethane (TCNQ) [19]. It has been shown that the ferrimagnetic behaviour increases with the increase of the degree of crystallinity of the polymer. In the present work we will analyse the possible sources of magnetic moments and the mechanism that will make them exhibit room temperature ferromagnetic behaviour.

2. Experimental details

Poly(3-methylthiophene) (P3MT) was electrochemically synthesized. Details of the synthesis in the oxidized state and subsequent reduction are described in [1]. Pellets were obtained using a pressure of 250 bar in an isostatic chamber, the powder being enclosed in a capsule of silicone ribbon. Magnetic measurements were performed using a Quantum Design SQUID magnetometer model MPMS-5S. After the measurements, a small piece of the sample (sample A), was encapsulated in a quartz tube containing argon for the ESR measurements performed using a Varian E-109 spectrometer equipped with an ESR Oxford cryostat. In order to study the room temperature ferromagnetic behaviour, as a function of the pressure used to make the pellets, we decided to work with polypyrrole. This allowed us to follow an easy chemical synthesis route without any magnetic component, resulting in a large amount of polymer powder. In this way, we could measure the powder and the pellets obtained for different pressures using equal amounts of the same powder, a task impossible to achieve with the small amounts of the electrochemically synthesized poly(3-methylthiophene) samples. Polypyrrole (PPy) was chemically prepared at 25 °C by the oxidation of pyrrole using ammonium persulfate in the proportion 3 of monomer to 1 of the oxidant. In a glass recipient 11.4 g of ammonium persulfate were dissolved in 100 ml of HCl (1 M). The persulfate was slowly added to the pyrrole solution. Room temperature $M \times H$ measurements were performed for the powder (sample B), the powder pressed uniaxially at 3.9 kbar (sample C) and at 9.5 kbar (sample D).

3. Results and discussion

3.1. Identifying the resonance

Figure 1 shows the extended X-band spectrum of sample A at 4.2 K. An enlargement is given to show the baseline contribution. The data were recorded with a microwave power of 20.2 mW, modulation amplitude of 0.1 G and attenuation of 25 db. Only a narrow line (∼10 G) close to $g = 2$ and attributed to the polymer can be observed in the full range. This result confirms the absence of contamination that has already been proved by atomic absorption analysis [20]. If a contaminant could be responsible for the ferromagnetic behaviour, the most probable one would be iron or iron oxides (especially magnetite). We have also to assume that these contaminants are segregated in large volume clusters because if they are dispersed as single particles they will give rise to paramagnetism and if they are assembled in small clusters they will show superparamagnetism. Based on the 300 K saturation magnetization value of 0.04 emu g^{-1} [1], 184 ppm of the sample mass of 8.2 mg should be iron, which has a saturation magnetization of 218 emu g^{-1} at 20 °C [21]. It could also be possible that 440 ppm will be magnetite, with saturation magnetization of 92 emu g^{-1} at 20 °C [21]. Those high values of contamination should show up in the ESR spectrum of figure 1. Isolated Fe^{3+} ions in a low symmetry environment are expected to be seen in the X-band with a g-value around 4.3. A $g = 2$ can also be observed due to iron or iron oxide

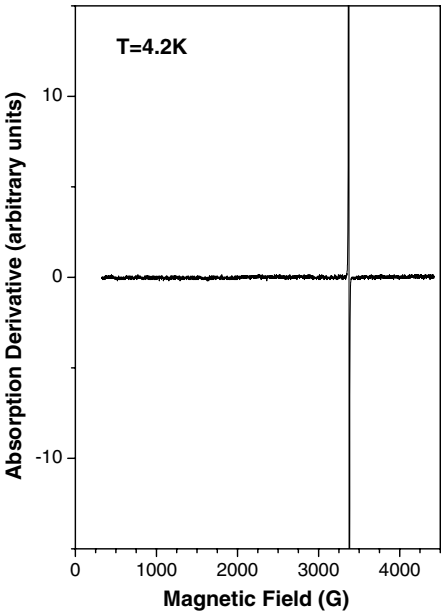

Figure 1. Extended X-band ESR spectrum of sample A at 4.2 K.

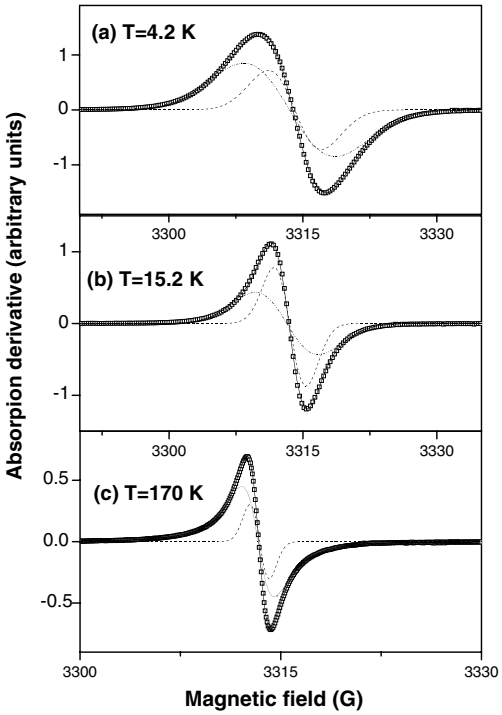

Figure 2. (a) and (b): ESR data fitted (full line) to a combination of a broad (dash and dotted line) and a narrow (dashed) Gaussian line. (c) ESR data fitted (solid line) to a combination of a broad (dash and dotted line) Lorentzian line and a narrow (dashed) Gaussian line.

clusters but with linewidths of 10^2–10^3 G [22]. No such lines can be observed in figure 1. In figure 2 the ESR spectra of sample A, seen in figure 1, are shown at 4.2, 15.2 and 170 K. The sample was inserted into the microwave cavity at 4 K and the experiment was performed raising the temperature until 286 K using a microwave power of 0.16 mW. For the ESR data at 15.2 K and below the linewidths could be fitted (solid line) using two Gaussian lines, with the broader line (dash and dotted line) at a slightly lower magnetic field than the other Gaussian (dotted line). From 20 K and above the best fittings were achieved using a Lorentzian (lower magnetic field) and a Gaussian line. It is interesting to discuss the possibilities of this Gaussian–Lorentzian change. The Gaussian shape could be due to unresolved fine or hyperfine structures, inhomogeneous magnetic field or interacting spins. Interacting spins, as in a ferromagnetic system, are expected to show a Gaussian shape. Each interacting spin will show a slightly different resonance frequency and the ESR line will be a sum of individual, sharper transitions [23]. If we have non-interacting spins, we expect to observe a Curie dependence of the intensity due to localized spins. Figure 3 shows intensities, g-values and linewidths for both lines from 4.2 to 286 K. The inset of figure 3(a) shows intensity as a function of inverse temperature $(1/T)$. If the spins were non-interacting, the expected behaviour should be a horizontal line, which is not observed. It is interesting to compare the ESR data of sample A with ESR data in the literature. X-band ESR measurements have been reported in films of BF_4^- doped poly(3-methylthiophene) [24]. For the 6.7 mol% the behaviour of the linewidth with temperature is similar to what we observed in figure 3(c). The lines are also composed of Lorentzian and Gaussian components, the Gaussian component decreasing with increasing doping level. The Gaussian line was ascribed to structural defects, although it is not clear which type of defect could be responsible for such a line. *In situ* ESR measurements in ClO_4^- doped films have also shown the combination of Lorentzian and Gaussian lines [25] showing again that the Gaussian component decreases and finally disappears when the doping level is increased. In [1] we have attributed the magnetic moments to the spin 1/2 polaronic defects formed into the polymer. Determining the number of spins 1/2 from the comparison of the room temperature ESR intensity with a standard, we have obtained the number of spins, in excellent agreement with the number of polarons inferred from the doping level (around 5%) obtained from electron dispersive x-ray spectroscopy (EDS) measurements. But, in order to compare the data with those of a standard for the number of spins, we implicitly assumed that we had a Curie behaviour in order to exactly cancel the $1/T$ dependence in both the sample and the standard. Of course, if we have interacting spins this is not true and we can consider that the value obtained is an approximation. In summary, we conclude that we are observing correlated polarons and we assume, in the same way as [14], that from the two polarons that interact to create a $S = 0$ or 1 bipolaron to the non-interacting polarons that show Curie behaviour, there are intermediate possible states of interaction that depend on the distance between the centre of each polaron. We assume that there is a critical distance, below which the interaction will render the line Gaussian.

3.2. Increasing the saturation magnetization with pressure

Some interesting conclusions can be obtained from the ESR analysis of the data. First, the two different g-values are probably related to different magnetic environments in the

Table 1. Parameters of the room temperature M versus H curves as a function of the pressure used to make the pellets.

Sample	M_S (emu g^{-1})	χ_{DP} (emu g^{-1} Oe^{-1})	M_R (emu g^{-1})	H_C (Oe)
B (powder)	—	-7.01×10^{-7}	—	—
C (3.9 kbar)	0.0046	-8.91×10^{-7}	2.7×10^{-4}	70
D (9.5 kbar)	0.0171	-1.13×10^{-6}	7.0×10^{-4}	45

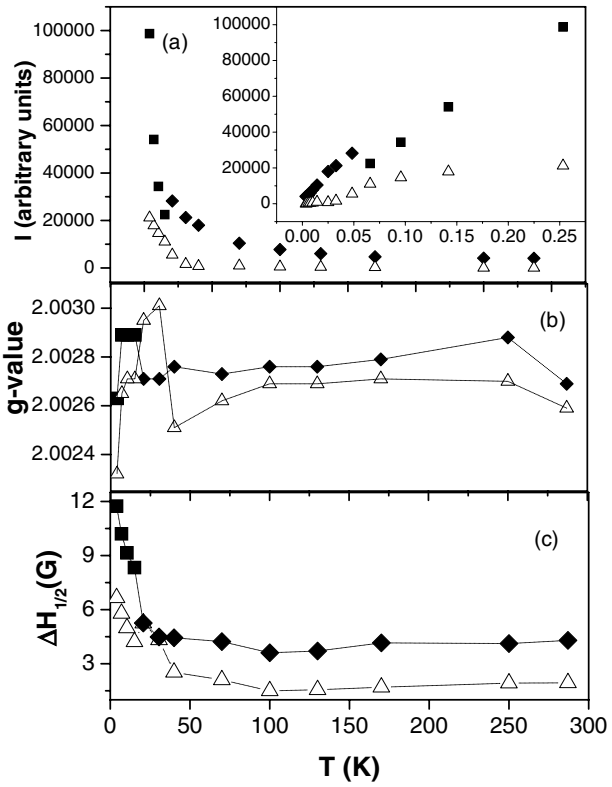

Figure 3. Intensities, g-values and linewidths versus temperature obtained from the fittings shown in figure 2. Full squares shows the behaviour of the broad Gaussian line that changes into a Lorentzian line (full diamonds) and open triangles the behaviour of the narrow Gaussian line. Inset: intensity versus inverse temperature ($1/T$).

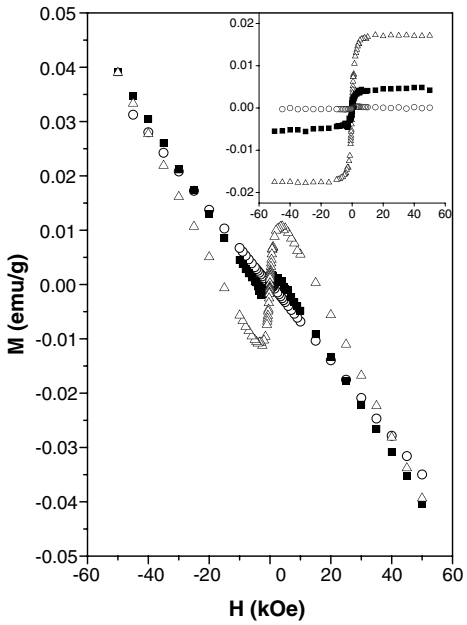

Figure 4. Magnetization versus magnetic field at 300 K. Sample B (open circles); sample C (full squares) and sample D (open triangles). Inset: saturation magnetization versus magnetic field at 300 K for the same samples.

polymer. In figure 3(a) we observe that the line that remains Gaussian until room temperature corresponds to the less intense line. We can speculate that this line comes from the more ordered regions of the polymer, or from the crystalline regions and that this is the part of the polymer that remains ferromagnetic at room temperature. This supposition is in agreement with what was observed in PANI–TCNQ in [19]. From x-ray diffraction data of our samples, the crystalline portion is low, being less than 10%. Now, if we focus only on the portion of the samples that remains ferromagnetic at room temperature, the data of figure 4 will be analysed. In figure 4 we show room temperature $M \times H$ curves for samples B (polypyrrole powder), C (powder pressed at 3.9 kbar) and D (powder pressed at 9.5 kbar). For sample B, the contribution is almost entirely diamagnetic, but this room temperature diamagnetic curve is the sum of positive and negative contributions. For samples C and D a ferromagnetic saturation magnetization is observed, with a tendency of the diamagnetic contribution to increase. The data for the three samples was fitted with equation (1):

$$M(H) = M_s + \chi_D H. \tag{1}$$

M_s stands for the saturated ferromagnetic contribution. χ_D is the diamagnetic contribution. The parameters are shown in table 1. Values for the remanent magnetization and coercive fields are also shown. In the inset of figure 4, the saturation magnetization contributions for the three samples are displayed.

For sample B no room temperature saturation magnetization could be obtained from the fitting, within the error. For samples C and D we observe an increase in the values of the saturation magnetization with increase of pressure. The increase in the diamagnetic contribution with pressure can be easily explained. The positive contribution contained in the diamagnetic term is decreased and some of the magnetic moments are observed in the ferromagnetic phase expressed in the saturation magnetization. The increase of the room temperature saturation magnetization with pressure suggests that pressure is contributing to increasing the crystalline portion of the pellet. The lack of saturation magnetization in powder is consistent with observation of true Curie behaviour in a powder of polyaniline by Sarifictci *et al* [26]. In the opposite direction, Chauvet *et al* [27] have observed a decrease of the EPR

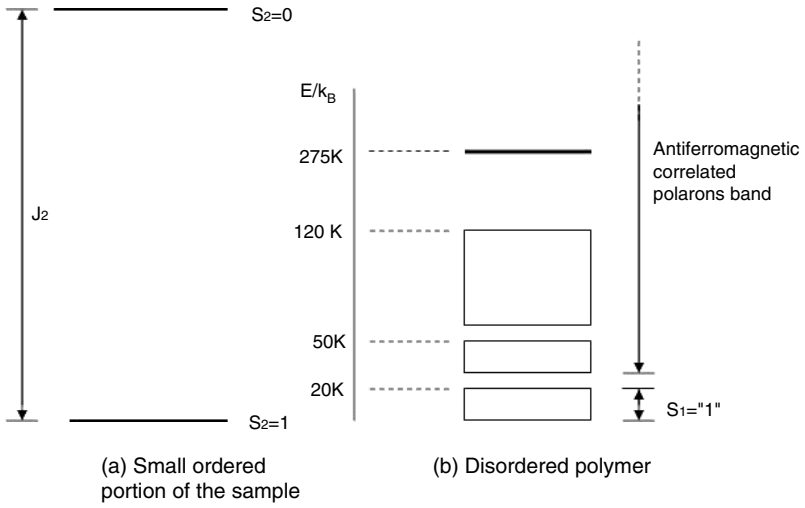

Figure 5. Model for a distribution of the energy levels; (a) for the triplet $S_2 = 1$ and singlet $S_2 = 0$ bipolarons in the crystalline regions. (b) For the ferromagnetically correlated $S_1 =$ '1' and antiferromagnetically correlated polaron bands in the disordered polymer.

intensity as a function of pressure in doped polypyrrole. They assumed that pressure would make excited triplet bipolarons less accessible, explaining the magnetic moments observed without pressure as due to polarons (Curie behaviour) and thermally accessed triplet bipolarons.

The couplings of similar pairs of spin 1/2 magnetic moments via the exchange interaction have been discussed by Abragam and Bleaney [28]. In zero magnetic field, in the condition of strong isotropic exchange, the triplet state is degenerate. With the application of a magnetic field no EPR transitions are expected between the singlet ($S = 0$) and triplet ($S = 1$) states. The ground state is determined by the sign of the exchange interaction J defined as $J = (E_T - E_S)$ where E_T and E_S are the energies of the triplet and singlet states respectively. If J is positive (antiferromagnetic coupling) the singlet is the ground state and if J is negative (ferromagnetic coupling) the triplet is the ground state. If ferromagnetic behaviour is observed at room temperature we expect J/k_B to be of order higher than room temperature. This condition of strong isotropic exchange implies that the isotropic exchange interaction is much higher than the Zeeman contribution. In this case, if ferromagnetic coupling of the spin 1/2 polarons is favoured, we expect the triplet state to be the ground state and the singlet the excited state. It is not clear in which way the ferromagnetic coupling is favoured. In [26] the recrystallization of the powder polyaniline samples shows for some of the samples obtained a susceptibility that increases when the temperature decreases (not exactly in a linear way) and from some other samples a decrease in the susceptibility below 10 K. For the first case, in the same way as the results that we have obtained for sample A discussed in the present work, the increase of magnetization with decrease of temperature is evidence that the $S = 1$ state is the ground state. For samples that show a decrease in the susceptibility for temperatures below 10 K the situation is different, because this decrease is evidence that the $S = 1$ state is an excited state and in this case the $S = 0$ state is the ground state. Disorder will introduce some additional complications to this simple picture because, in the disordered region of the polymer complete ferromagnetic and antiferromagnetic coupling is prevented and we will assume that we have bands of ferromagnetic and antiferromagnetic coupled polarons. The higher the state into the band, the higher the coupling energy. A tentative scheme for such a situation, including both the small ordered crystalline region that we call region 2 and the disordered region 1, is shown in figure 5.

3.3. Understanding low magnetic field ESR and SQUID data

Let us try to understand our ESR and SQUID data, with the help of figure 5. In order to analyse the ESR data, we will discuss the influence of the Zeeman term in the $S_2 = 1$ and $S_1 =$ '1' triplet states. As discussed in [28] the effect of the magnetic field is to split the degenerate triplet levels and, in the condition of isotropic exchange, two superposed transitions within the triplet with $\Delta M = \pm 1$ will be expected. The low intensity data shown in figure 3(a) (open triangles) of the Gaussian ESR line corresponds to the two superposed transitions of the triplet state $S_2 = 1$. The high intensity data (closed squares) of the Gaussian ESR line correspond to the transitions of the $S_1 =$ '1' band of ferromagnetically correlated polarons, which makes a transition to high energy antiferromagnetically correlated polarons (Lorentzian line) around 20 K. Figure 6 shows (field cooling) FC and (zero field cooling) ZFC curves for 10 kOe (a) and 1 kOe (b). From figure 6(b) we can see the ferromagnetic–antiferromagnetic correlated polaron transition around 20 K in the ZFC curve. We can also see an increase in the magnetization curve, with different derivatives, associated with the progressive population of antiferromagnetically correlated polaron bands as the temperature is increased. In the case of the FC curve, we have a different situation. The magnetic field works against disorder in the direction of lining up the individual polarons with the magnetic field, contributing to the

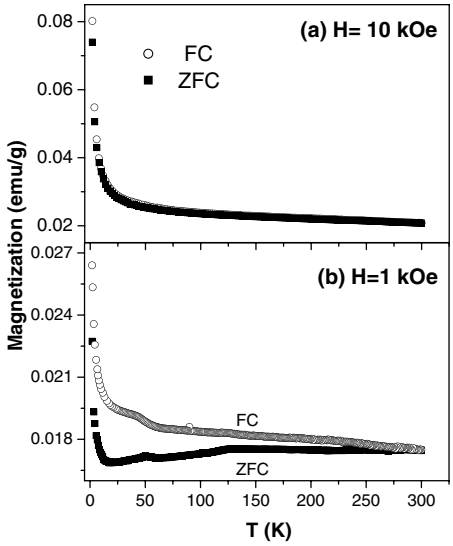

Figure 6. Magnetization versus temperature curves: ZFC (full squares) and FC (open circles). (a) For an applied field of 10 kOe. (b) For an applied field of 1 kOe.

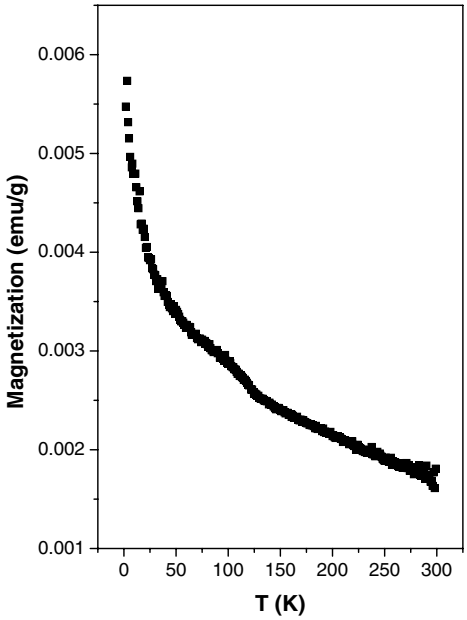

Figure 7. Spontaneous magnetization versus temperature. The sample was cooled without a magnetic field from 300 to 1.8 K. At 1.8 K a magnetic field of 50 000 Oe was applied for 10 min and then removed and the data were recorded with increasing temperature.

increase of the net magnetization in both ferromagnetically and antiferromagnetically correlated polaron bands.

3.4. Understanding high magnetic field SQUID data

When a high magnetic field is applied, two things happen. The splits of $S = 1$ triplet states are larger, and, in the disordered region, the magnetic field promotes an overlap of the ferromagnetically coupled and antiferromagnetically coupled polaron bands. At low temperatures, the main contribution is from the $S = 1$ triplet states. At high temperatures, the bands overlap will mask all the structure of different bands observed at low magnetic fields. Those differences are clear when we compare figures 6(a) and (b).

3.5. Understanding spontaneous magnetization SQUID data

In [1] we have discussed the influence of the applied magnetic field on the shape of the spontaneous magnetization curve. For low magnetic field (500 Oe) a convex behaviour very close to that expected from Weiss mean field theory and fitted to a $T^{-3/2}$ dependence was achieved. For higher fields (5000 Oe), the curve showed a more linear behaviour and was fitted to a T^{-1} behaviour. From the fitting of both curves a critical temperature of approximately 815 K (T_{C2}) was obtained. We would like to understand the spontaneous magnetization data using our scheme described in figure 5. When the magnetic field is small there is no overlap of polaron bands in the disordered region, promoted by the magnetic field, and the main contribution at low temperature is from the $S = 1$ states of both regions (1 and 2) of the polymer. The contribution of region 1 is unsaturated and the contribution of region 2 only disappears when the J_2 value is reached. This situation corresponds to finding a zero magnetization because the $S_2 = 0$ state has been reached. From the point of view of the decrease of the spontaneous magnetization, it would be equivalent to the fitted value of (T_{C2}). In figure 7, we show spontaneous magnetization as a function of temperature for sample A, magnetized using a magnetic field of 50 000 Oe. The sample was cooled without a magnetic field from 300 to 1.8 K. At 1.8 K the magnetic field was applied for 10 min and then removed. Now, the situation is completely different. The magnetic field promotes an overlap of the antiferromagnetically and ferromagnetically correlated polaron bands and the final magnetization after the application of the magnetic field is a superposition of ferromagnetic and antiferromagnetic polarons. The lower the energy of the interaction state the higher the population at 1.8 K. As the temperature increases, the lower energy states relax the magnetization and when the temperature increases, other higher energy interactions start to relax their magnetization.

3.6. Understanding M versus H SQUID data

As discussed above, in the high magnetic field limit, ferromagnetic and antiferromagnetic polaron bands are superposed. But we can assume that at 5 K, the contribution of region 1 comes mainly from the $S_1 =$ '1' states. We also assume that the $S_2 = 1$ states have a saturated behaviour at 5 K, and we represent it by a constant M_{s2} at high magnetic fields. Then, representing the magnetization of the disordered region with a contribution of states with the magnetic field parallel and antiparallel to the magnetic moment μ_1 we write for the magnetization:

$$M = M_1(\exp(\beta\mu_1 H) - \exp(-\beta\mu_1 H))/(1 + \exp(\beta\mu_1 H) + \exp(-\beta\mu_1 H)) + M_{s2}. \quad (2)$$

We have used $\beta = 1/k_B$ T. The 5 K $M \times H$ SQUID data are shown in figure 8 (open circles) with the high field

Table 2. Fitting parameters of magnetization data as a function of the magnetic field.

T (K)	M_1 (emu g^{-1})	M_{s2} (emu g^{-1})	χ_D (emu g^{-1} Oe^{-1})	μ_1 (emu)
5	1.35×10^{-1}	3.7×10^{-2}	—	2.17×10^{-20}
300	—	0.04	-1.95×10^{-6}	—

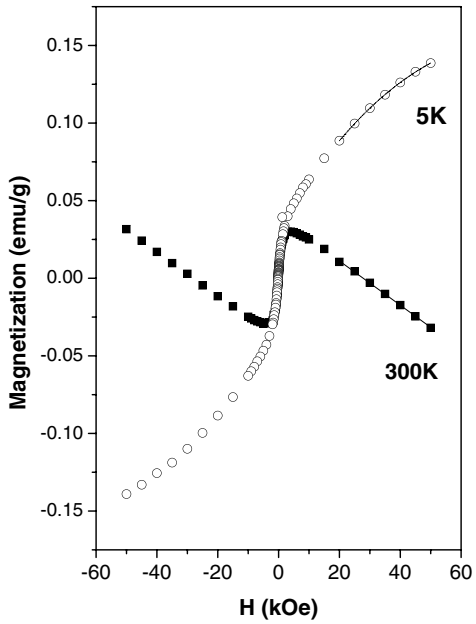

Figure 8. Magnetization versus magnetic field. At 300 K (full squares) and 5 K (open circles). The dashed line is a fitting to equation (2). The solid line is a fitting to equation (1).

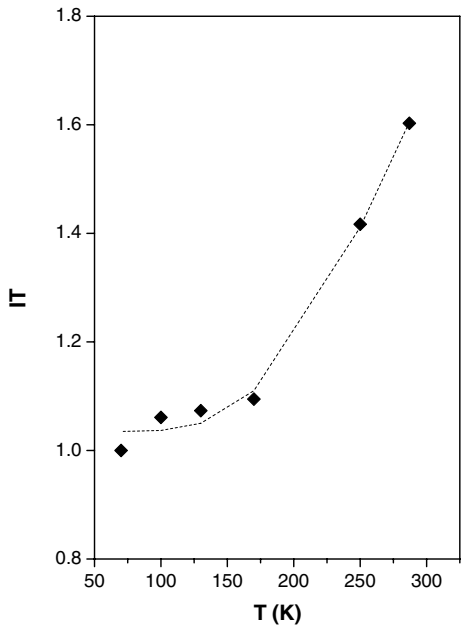

Figure 9. (Full diamonds) Replot of the most intense line of figure 3(a) in the range 70–286 K in the form of intensity times temperature versus temperature (IT versus T). The data are normalized using the 70 K value and fitted (dashed line) using equation(3).

data (20–50 kOe) fitted (dashed line) with equation (2). For the 300 K magnetization data (full squares), a linear fit of the high field data was performed using equation (1) (full line), with M_s representing the contribution from region 2. The fitted parameters are shown in table 2.

Taking into account all the above-mentioned limitations and also considering that actually the values of M_1 and μ_1 are field dependent due to overlap of the polarons bands, these values should be taken with care. The important point is that, although there are limitations of the model, the values of M_{s2} are roughly the same at 5 or 300 K. This result is in agreement with the fact that it comes from the $S_2 = 1$ triplet.

3.7. An estimation of J_1 from ESR data

If we return now to the analysis of the ESR data of figure 3(a), based on the model discussed in figure 5, we observe that the decrease observed in the low intensity Gaussian ESR line only reflects the thermal population of the $S_2 = 1$ triplet states. The microwave magnetic field induces transitions between states i and j. There will be an absorption of energy since in general the state of lower energy normally has a greater population, and the total number of transitions in either direction is proportional to the population of the initial state [28]. Then, as the temperature increases, the lower levels of the triplet become progressively depopulated and the absorption decreases. On the other hand, the increase of the high intensity ESR Lorentzian line, reflects the thermal population of bands with progressively less antiferromagnetically correlated polarons. In this way, we can use it for a crude estimation of the exchange constant J_1 of the disordered part of the polymer. We have to keep in mind that we are estimating the second exchange constant of the amorphous phase because the first constant is associated with the transition from ferromagnetically correlated to antiferromagnetically correlated polaron bands that took place around 20 K. In figure 9 we replot the data of the most intense ESR Lorentzian line in figure 3(a) as intensity times temperature, (IT) versus T. We assume that all correlated polarons in the antiferromagnetically correlated bands have the same exchange energy J_1. In this way we take only the contribution of the high energy bands, using the normalized data in the range 70–286 K, and we write for normalized IT:

$$IT = 4C_a/(3 + \exp(J_1/k_B T)) + C_b. \quad (3)$$

Here C_a and C_b are the Curie constants representing interacting and non-interacting polarons. In the limit of $J_1 \ll k_B T$, the Curie behaviour is recovered. The fitting of the normalized data yields a positive $J_1/k_B = 891$ K (dashed line) with $C_a = 3.60$ and $C_b = 1.03$. This means that with our model of fixed J_1, we find about 29% of non-interacting polarons. In

spite of the scatter of the data and the fact that this is a crude estimation, it is interesting to note that the J_1 value is close to the J_2 value or $T_C = 815$ K obtained from another sample in [1].

4. Conclusions

In this work the ferromagnetic behaviour of partially doped poly(3-methylthiophene) is revised. Instead of the Dzialoshinsky–Morya mechanism of weak ferromagnetism, we now assume that the mechanism that gives rise to the room temperature ferromagnetism is the ferromagnetic coupling of polarons to create a triplet bipolaron. Our basic assumption is that the magnetic moments are spin 1/2 polarons that can interact antiferromagnetically and/or ferromagnetically. In the crystalline region, the interaction gives rise to $S = 0$ and 1 bipolarons, as emphasized by Bussac and Zuppiroli [14]. If the $S = 1$ triplet state is lower in energy, the crystalline region will show ferromagnetic behaviour. In the disordered region, disorder will prevent the complete $S = 1$ and 0 coupling and bands of polarons ferromagnetically and antiferromagnetically coupled will appear. Using this approach (summarized in figure 5), we are able to qualitatively explain all our ESR and SQUID data. The role played by pressure in our pellets is to contribute to increasing the crystalline portion of the polymer. The doping level also plays a role not only in the generation of the defects but also in affecting the plasticity of the polymer. New ESR data have shown that we can once more disregard contamination by magnetic impurities. The intrinsic character of this magnetic behaviour opens new opportunities of applications of conduction polymers in magnetic devices. One of them is the possibility of beating the superparamagnetic limit when magnetic nanoparticles are dispersed in a conducting polymer. This fact has already been demonstrated by Yang *et al* [29] and Poddar *et al* [30] when those authors, instead of observing superparamagnetism as they expected, assuming the conducting polymer to be a diamagnetic matrix, observed ferromagnetism at room temperature.

Acknowledgments

This work was partially supported by Fundação de Amparo à Pesquisa do Estado de São Paulo (FAPESP) and Conselho Nacional de Desenvolvimento Científico e Tecnológico (CNPq).

References

[1] Nascimento O R, de Oliveira A J A, Correa A A, Bulhões L O S, Pereira E C, Souza V M and Walmsley L 2003 *Phys. Rev.* B **67** 144422
[2] Bertho D and Jouanin C 1987 *Phys. Rev.* B **35** 626
[3] Bredas J L, Scott J C, Yakushi K and Street G B 1984 *Phys. Rev.* B **30** 1023
[4] Su W P, Schrieffer J R and Heeger A J 1979 *Phys. Rev. Lett.* **42** 1698
Su W P, Schrieffer J R and Heeger A J 1980 *Phys. Rev.* B **22** 2099
[5] Fisher A J, Hayes W and Wallace D S 1989 *J. Phys.: Condens. Matter* **1** 5567
[6] Bertho D, Jouanin C and Lussert J M 1988 *Phys. Rev.* B **37** 4039
[7] Wohlgenannt M, Jiang X M and Vardeny Z V 2004 *Phys. Rev.* B **69** R241204
[8] Nalwa H S 1989 *Phys. Rev.* B **39** 5964
[9] Mizoguchi K, Kachi N, Sakamoto H, Kume K, Yoshioka K, Masubuchi S and Kazama S 1997 *Synth. Met.* **84** 695
[10] Kahol P K and Mehring M 1986 *Synth. Met.* **16** 257
[11] Kahol P K, Pinto N J and McCormick B J 1994 *Solid State Commun.* **91** 21
[12] Kahol P K, Raghunathan A, McCormick B J and Epstein A J 1999 *Synth. Met.* **101** 815
[13] Mizoguchi K, Nechtschein M, Travers J-P and Menardo C 1989 *Phys. Rev. Lett.* **63** 66
[14] Bussac M N and Zuppiroli L 1993 *Phys. Rev.* B **47** 5493
[15] Kahol P K, Spencer W R, Pinto N J and McCormick B J 1994 *Phys. Rev.* B **50** 18647
[16] Kahol P K, Raghunathan A and McCormick B J 2004 *Synth. Met.* **140** 261
[17] Zuppiroli L, Bussac M N, Paschen S, Chauvet O and Forro L 1994 *Phys. Rev.* B **50** 5196
[18] Long Y, Chen Z, Shen J, Zhang Z, Zhang L, Xiao H, Wan M and Duvail J L 2006 *J. Phys. Chem.* B **110** 23228
[19] Zaidi N A, Giblin S R, Terry I and Monkman A P 2004 *Polymer* **45** 5683
[20] Pereira E C, Correa A A, Bulhões L O S, Aleixo P C, Nóbrega J A, de Oliveira A J A, Ortiz W A and Walmsley L 2001 *J. Magn. Magn. Mater.* **226** 2023
[21] Cullity B D 1972 *Introduction to Magnetic Materials* (Reading, MA: Addison-Wesley) p 129
[22] Duttine M, Villeneuve G, Poupeau G, Rossi A M and Scorzelli R B 2003 *J. Non-Cryst. Solids* **323** 193
[23] Bencini A and Gateschi D 1990 *Electron Paramagnetic Resonance of Exchange Coupled Systems* (Berlin: Springer) p 137
[24] Schärli M, Kiess H, Harbeke G, Berlinger W, Blazey K W and Müller K A 1988 *Synth. Met.* **22** 317
[25] Harima Y, Eguchi T, Yamashita K, Kojima K and Shiotani M 1999 *Synth. Met.* **105** 121
[26] Sariciftci N S, Heeger A J and Cao Y 1994 *Phys. Rev.* B **49** 5988
[27] Chauvet O, Sienkiewicz A, Forro L and Zuppiroli L 1995 *Phys. Rev.* B **52** R13118
[28] Abragam A and Bleaney B 1986 *Electron Paramagnetic Resonance of Transitions Ions* (New York: Dover) p 502
[29] Yang Q L, Zhai J, Feng L, Song Y-L, Wan M-X, Jiang L, Xu W-G and Li Q S 2003 *Synth. Met.* **135** 819
[30] Poddar P, Wilson J L, Srikanth H, Morrison S A and Carpenter E E 2004 *Nanotechnology* **15** S570